

Superradiant to subradiant phase transition in the open system Dicke model: Dark state cascades

Michael Gegg,^{1,*} Alexander Carmele,¹ Andreas Knorr,¹ and Marten Richter¹

¹*Institut für Theoretische Physik, Nichtlineare Optik und Quantenelektronik,
Technische Universität Berlin, Hardenbergstr. 36, EW 7-1, 10623 Berlin, Germany*

(Dated: October 11, 2024)

Resonantly driven two-level systems in the bad cavity limit (short photon lifetime) have been studied under the name cooperative resonance fluorescence. This system exhibits a nonequilibrium phase transition for both total spin preserving and nonpreserving quantum master equations. We study the spin nonpreserving case beyond the bad cavity limit and show that the nature of the phase transition is changed: while in the bad cavity limit subradiant states are actively suppressed below and above the phase transition, these states experience suppression below and amplification above the phase transition in the good cavity limit. Hence the system changes from a predominantly superradiant into a predominantly subradiant phase at the transition. Experimentally accessible signatures of this effect as well as entanglement properties of the system are discussed. A cascade of dark Dicke states is generated when we switch off the drive and let the system relax into the ground state.

The open (and closed) system Dicke model has been a work horse in quantum optics and beyond for decades [1–22]. Current research on Dicke model based systems includes novel laser-like systems [18], phase transitions [15, 22], quantum information and super/subradiance [10, 13, 19, 20, 23]. In recent years superradiance has been investigated with respect to entanglement [19] and subradiance for its prospects to store quantum information [20, 23]. The Dicke model assumes N identical two-level systems, interacting with a bosonic cavity mode. In a straight forward approach the master equation scales exponentially in the number N of two-level systems, rendering simulations for large N impossible. Context dependent limits and approximations for both analytical and numerical treatments address this problem [4–8, 10, 13]. Usually for superradiance total spin conservation (explained below) is assumed, neglecting subradiant states. This reduces the numerical complexity to $\sim N^2$ [13] or sometimes even allows analytic solutions [7, 8]. However, ubiquitous phenomena like decay processes and pure dephasing break this symmetry. Therefore realistic treatments – including subradiant effects – require a different methodology.

Symmetries in these master equations reduce the complexity from exponential in N to $\sim N^3$, even without total spin conservation [18, 22, 24–26]. This makes exact calculations for moderate emitter numbers feasible and removes constraints imposed by assumptions and approximations. Furthermore the method can be applied to any permutationally symmetric multi-level system setup [24].

In this letter we investigate the population of subradiant states through decay and pure dephasing processes – both do not conserve the total spin. Counterintuitively, the cavity lifetime determines the population of the subradiant states. Increasing the cavity lifetime changes the nature of a nonequilibrium phase transition, amplifying

subradiant states. Experimentally accessible signatures and entanglement properties via spin squeezing are discussed. Switching off the external driving, the subsequent relaxation into the ground state forms a long-lived cascade of dark Dicke states.

We consider the usual Dicke model. Additionally the TLS are driven by an identical, classical optical, cw field E . Driving is necessary since subradiant states are excited states. In a frame rotating at the external laser frequency, using the rotating wave approximation the system Hamiltonian reads

$$H = \Delta_0 b^\dagger b + \Delta_1 J_{11} + g(J_{10}b + J_{01}b^\dagger) + E(J_{10} + J_{01}),$$

where Δ_0, Δ_1 are the mode and TLS detuning, g is the TLS-mode coupling, E is the optical driving, b, b^\dagger are photonic operators and $J_k = \sum_i \sigma_k^i$, $k = 11, 10, 01, 00$ are the collective spin operators. Excited and ground state of the individual TLS are $|1\rangle_i, |0\rangle_i$, the lower indices of the spin operators represent the Ket and Bra notation: $\sigma_{11}^i = |1\rangle_i \langle 1|_i$, $\sigma_{10}^i = |1\rangle_i \langle 0|_i$, $\sigma_{01}^i = |0\rangle_i \langle 1|_i$

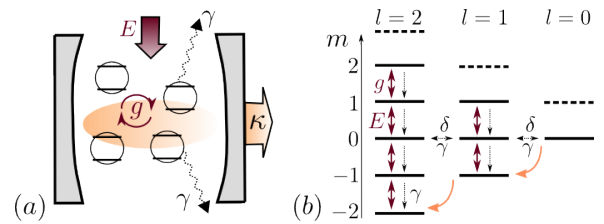


Figure 1. (a) Schematic representation of the system. (b) Dicke states for $N = 4$. The lowest state in each l subspace is dark – the lowest state in the superradiant $l_{max} = N/2$ subspace is the ground state. The interactions are depicted: Hamiltonian part (purple, thick), dissipators \mathcal{D}_{de} and \mathcal{D}_{pd} (black, thin) and dark state cascade (orange, curved). Dashed lines indicate the additional states for $N = 5$ (with different values of m, l).

and $\sigma_{00}^i = |0\rangle_i\langle 0|_i$. We assume resonant excitation field, cavity and TLS. Both cavity and TLS are subject to loss and dephasing, using Lindblad formalism [27]. The master equation reads

$$\partial_t \rho = \mathcal{L} \rho = \frac{i}{\hbar} [\rho, H] + \mathcal{D}_{de} + \mathcal{D}_{pd} + \mathcal{D}_{ph}. \quad (1)$$

The Lindblad dissipators describe decay processes like radiative and non-radiative decay $\mathcal{D}_{de} = \gamma/2 \sum_i (2\sigma_{01}^i \rho \sigma_{10}^i - \sigma_{11}^i \rho - \rho \sigma_{11}^i)$, pure dephasing $\mathcal{D}_{pd} = \delta/2 \sum_i (\sigma_z^i \rho \sigma_z^i - \rho)$ and cavity decay $\mathcal{D}_{ph} = \kappa/2 (2b\rho b^\dagger - b^\dagger b\rho - \rho b^\dagger b)$, see Fig. 1 (a). We use $\sigma_z^i = \sigma_{11}^i - \sigma_{00}^i$. All contributions to the master equation except \mathcal{D}_{de} and \mathcal{D}_{pd} are total spin preserving, (Fig. 1 (b)). The total spin $l(l+1)$ is the eigenvalue of the $J^2 = (J_{10}J_{01} + J_{01}J_{10})/2 + J_z$ operator, with $J_z = 1/2 \sum_i \sigma_z^i$. The J^2 and J_z eigenvalues determine the coupling strength of the multi TLS (Dicke) state to an optical mode, the collective dipole transition element. This coupling strength distinguishes between superradiance and subradiance. For superradiant states the dipole element scales superlinear in N , while for subradiant states the scaling is sublinear in N and some subradiant states are dark [28]. Dark means that the dipole transition element vanishes, meaning these states cannot decay e.g. creating a cavity photon. However these states still decay into other states via the decay and dephasing processes \mathcal{D}_{de} and \mathcal{D}_{pd} acting individually on the emitters, c.f. Fig. 1 (b). Generally the spin preserving contributions in the master equation generate quantum correlations leading to collective TLS behavior (such as super- and subradiance) and the nonpreserving terms destroy correlations leading to individualization. However only the spin nonpreserving contributions introduce coupling between superradiant and subradiant states, thus in order to prepare subradiant states an interplay of collectivity and individualization is necessary. In the bad cavity limit ($\kappa \gg g$) Eq. (1) corresponds to the cooperative resonance fluorescence setup [4, 5]. The system exhibits a non-equilibrium phase transition for increasing E for both total spin preserving and nonpreserving setups [4]. For moderate cavity lifetimes ($\kappa \sim g$) the system resembles the absorptive optical bistability setup [29] (instead of driving the TLS, in optical bistability the cavity is driven, opposed to Fig. 1 (a)). Besides the steady state, density matrix states with very long lifetimes can exist, which lead to the observation of bistabilities in experiments with finite measurement time [30]. In some limits these lifetimes become infinite, resulting in a second steady state. For optical bistability these long lifetimes are called tunneling times [31, 32], more general this phenomenon is called dissipative phase transition [33].

Investigating super- and subradiant states requires a suitable measure. Unfortunately computing the respective Dicke state populations is not sufficient if

dephasing is present: Dicke states $|l, m\rangle$ are eigenstates of J^2 and J_z with corresponding quantum numbers $l(l+1)$, $0 \leq l \leq N/2$ and $|m| \leq l$. $l_{max} = N/2$ defines the superradiant subspace and $l_{min} = 0, 1/2$ defines the (most) subradiant subspace, see Fig. 1 (b). Consider the $N = 2$ Dicke (or Bell) states: The superradiant subspace consists of three states $|1, -1\rangle$, $|1, 0\rangle$, $|1, +1\rangle$ while the subradiant subspace consists of a single dark state $|0, 0\rangle$. Please note that $|1, 0\rangle$ and $|0, 0\rangle$ have the same number of excitations. First we calculate the population: $\text{tr}[|l, m\rangle\langle l, m| \rho] = \langle |l, m\rangle\langle l, m| \rangle = p(l, m)$. We will use the method from Refs. 18 and 24. With this the expectation values are $p(1, -1) = \mathcal{P}[0, 0, 0]$, $p(1, 0) = 1/2(\mathcal{P}[1, 0, 0] + \mathcal{P}[0, 1, 1])$, $p(1, 1) = \mathcal{P}[2, 0, 0]$ and $p(0, 0) = 1/2(\mathcal{P}[1, 0, 0] - \mathcal{P}[0, 1, 1])$, using the trace condition of Ref. 26. For $N = 2$ we get $\mathcal{P}[0, 0, 0] = \langle \sigma_{00}^1 \sigma_{00}^2 \rangle$, $\mathcal{P}[1, 0, 0] = \langle \sigma_{11}^1 \sigma_{00}^2 + \sigma_{00}^1 \sigma_{11}^2 \rangle$, $\mathcal{P}[2, 0, 0] = \langle \sigma_{11}^1 \sigma_{11}^2 \rangle$, $\mathcal{P}[0, 1, 1] = \langle \sigma_{10}^1 \sigma_{01}^2 + \sigma_{01}^1 \sigma_{10}^2 \rangle$. Generally $\mathcal{P}[i, 0, 0]$ is the probability of finding i excitations in the system, for $j, k \neq 0$ $\mathcal{P}[i, j, k]$ represents a quantum coherence. The indices i, j, k obey $0 \leq i + j + k \leq N$. Thus increasing N increases possible combinations, however the generalization is straightforward. Dicke state expectation values read $p(l, m) = a_0(l, m)\mathcal{P}[n, 0, 0] \pm a_1(l, m)\mathcal{P}[n-1, 1, 1] \dots$, with $n = m + N/2$. For a detailed introduction to this method see Ref. 24.

Preparing two TLS in the superradiant state ($p(1, 0) = 1$) implies a suppression of the subradiant state of equal excitation ($p(0, 0) = 0$) and thus $\mathcal{P}[1, 0, 0] = \mathcal{P}[0, 1, 1]$. All quantum coherences dephase due to system bath interactions, we illustrate this for pure dephasing e.g. $\partial_t \mathcal{P}[n, k, k] \propto -2k\delta\mathcal{P}[n, k, k]$. If for $p(1, 0) = 1$ dephasing is strong enough to completely suppress coherences, i.e. $\mathcal{P}[0, 1, 1] = 0$, while maintaining the excitation $\mathcal{P}[1, 0, 0] = 1$, the super and subradiant projectors yield $p(1, 0) = p(0, 0) = 1/2$.

For higher numbers of TLS, $\mathcal{P}[n, 0, 0]$ distributions allow a large variety of populations in super- and subradiant states even if quantum coherences are absent. Generally – when spin non-conserving terms are included – the superradiant subspace population decreases, since for large N the superradiant subspace is very small compared to the full Hilbert space. However without quantum coherences in the TLS basis the label super- and subradiance becomes meaningless since the quantum coherences are the collectivity of the Dicke states and reflect the redistribution of oscillator strength. Thus – in the open Dicke model – $\mathcal{P}[n-k, k, k]$ are the key quantities that distinguish a super- or subradiant state from a classical, incoherent mixture of TLS population ($\mathcal{P}[i, j, k] = 0$ for $j, k \neq 0$). The decay process \mathcal{D}_{de} acts individually and analogously results in incoherent mixtures.

It is therefore preferable to look at the ratio between

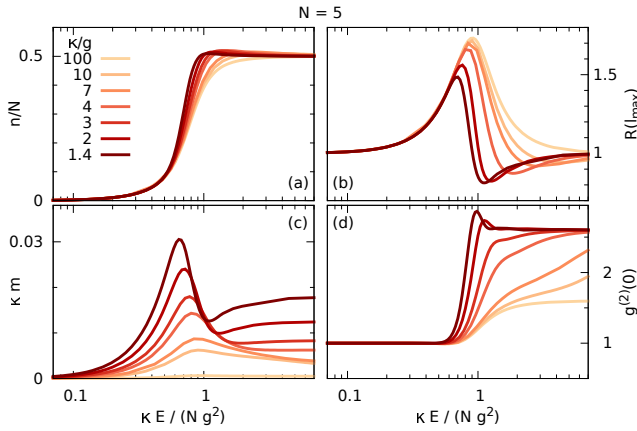


Figure 2. Variation of the external pumping strength for different ratios κ/g : (a) the normalized TLS excitation number $n/N = \langle J_{11} \rangle / N$, (b) the relative superradiant subspace occupation $R(l_{max} = N/2)$, (c) the cavity output rate $\kappa m = \kappa \langle b^\dagger b \rangle$ and (d) the photonic second order correlation function $g^{(2)}(0)$: Drastic qualitative change for κ/g approaching unity.

the full Dicke subspace population and its incoherent part $R(l) = \sum_m p(l, m) / (\sum_m a_0(l, m) \mathcal{P}[m + N/2, 0, 0])$. $R(l) = 1$ holds if the influence of quantum correlations between the TLS on the subspace population is zero or negligible – the TLS act *individually*. $R(l) < 1 / R(l) > 1$ holds if quantum correlations *suppress/increase* the respective subspace occupation – the TLS act *collectively*. $R(l)$ provides a reality check, since in any experiment dephasing is present and isolated Dicke subspaces (or states) never occur.

We solve Eq. (1) with our computer library PsiQuaSP [34] for master equations with reduced, polynomial scaling as described in Ref. 24. We use eigensolvers and time integration from PETSc and SLEPc [35–38].

We use $\gamma = 1.0 \text{ ns}^{-1}$ and $g = 3.3 \text{ meV}$ throughout this work. First pure dephasing is neglected, its influence is investigated later. Including small pure dephasing preserves all effects.

The most basic feature of the nonequilibrium phase transition is the change in steady state from ground state to a half excited TLS state with increasing external driving field (Fig. 2 (a)). A drastic change is seen in the relative superradiant subspace population $R(l_{max} = N/2)$, Fig. 2 (b). While in the bad cavity limit the superradiant subspace population is always increased by collective effects ($R(l_{max}) \geq 0$), we observe an increased suppression ($R(l_{max}) < 0$) of the superradiant subspace for decreased κ/g . This is accompanied by a drastic increase of coherent cavity photons below and a pronounced bunching at moderate photon numbers above the phase transition (Fig. 2 (c) and (d)). The maximum in the second order photon correlation function indicates the transition point from increased to suppressed superradiant subspace occupation. Please

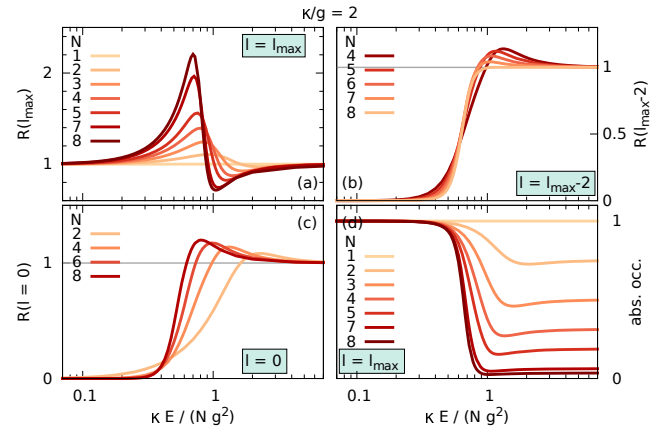


Figure 3. Relative Dicke subspace occupation for (a) the superradiant subspace $l = N/2$, (b) $l = N/2 - 2$, (c) $l = 0$. These states have no interactions due to the Hamiltonian. They only couple to states with $l > 0$ through decay and dephasing. (d) Absolute occupation in the superradiant subspace: Approaching zero above the phase transition for $N \rightarrow \infty$, even without correlations.

note that the cavity decay does not lead to an effective pure dephasing contribution for the TLS.

Above the phase transition collectivity favors the most subradiant subspace l_{min} : The dependence of $R(l_{max})$ on the number of TLS N , Fig. 3 (a), shows a growing collective change in population of the superradiant subspace for increasing N . In Fig. 3 (b) the ratio $R(l_{max} - 2)$ is plotted – it switches from suppressed below to increased above the transition. However the collective increase in population decreases for increasing N . For $N = 4, 5$ $l_{max} - 2$ corresponds to the most subradiant subspace i.e. $N = 4$: $l_{min} = 4/2 - 2 = 0$ and $N = 5$: $l_{min} = 1/2$. In these two cases the collective increase in population is strongest. For larger N subspaces with smaller l exist, e.g. $N = 6$: $l_{min} = l_{max} - 3$. Looking at $R(0)$ (only defined for even N), Fig. 3 (c), we see that the increase due to collective effects increases with N . Hence the collective increase is always most pronounced in the most subradiant subspace (l_{min}) above the phase transition. Remarkably, below the phase transition the subradiant subspaces are completely suppressed, c.f. Figs. 3 (b), (c).

The total occupation in the superradiant subspace tends to zero above the phase transition for $N \rightarrow \infty$, Fig. 3 (d). Naively we could associate this with subradiance. However for $E \rightarrow \infty$ the TLS are in a completely incoherent, equipartitioned state [39] and the superradiant subspace is only depopulated since this subspace becomes very small compared to the full Hilbert (Liouville) space for large N . This is clearly not a collective effect. This illustrates that (in the steady state) it is impossible to distinguish between collective and individual behavior by Dicke state occupations

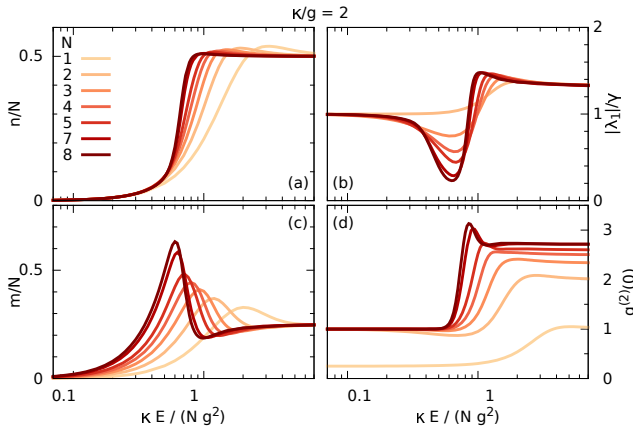


Figure 4. Experimental signatures for different N : (a) the normalized TLS excitation number $n/N = \langle J_{11} \rangle/N$, (b) the renormalized Liouvillian gap $|\lambda_1|/\gamma$, (c) the rescaled intracavity photon number $m/N = \langle b^\dagger b \rangle/N$ and (d) the second order correlation $g^{(2)}(0)$.

alone. However by looking at both the absolute and relative populations we conclude that in the good cavity and large N limit the system changes from a predominantly superradiant to a predominantly subradiant state at the phase transition. This constitutes the main result of this letter.

In Fig. 4 the N scaling of experimentally more accessible quantities is presented: The normalized TLS excitation develops a kink for increasing N , indicating a second-order transition, Fig. 4 (a). The smallest nonzero eigenvalue λ_1 of the Liouville operator \mathcal{L} (c.f. Eq. (1)), which corresponds to the slowest time scale in the system to reach steady state, decreases around the phase transition for increasing N , Fig. 4 (b). It might even vanish for $N \rightarrow \infty$, creating a second steady state. The intracavity photon number shows the formation of a local minimum at the transition and an increase in the peak intensity, Fig. 4 (c). Also bunching ($g^{(2)}(0) > 1$) increases for increasing N , Fig. 4 (d). Overall the transition becomes sharper and more pronounced for increasing N and decreasing κ/g , since these parameters increase the system size. This displays a typical property of phase transitions, which are well defined only in the thermodynamic limit (infinite system size) and blur for small system sizes [4, 40, 41].

Robustness test: So far all results were presented without including pure dephasing. In Fig. 5 (a) we see that the collective behavior of the relative Dicke subspace population is reduced for increasing δ . However the effect of clear distinction of superradiant state below and subradiant state above phase transition is preserved for $\delta \sim \gamma$. The general trend of Dicke subspace occupation is not affected by pure dephasing, as in Fig. 3 (d).

In the spin preserving setup the TLS are entangled via spin squeezing below the phase transition [13].

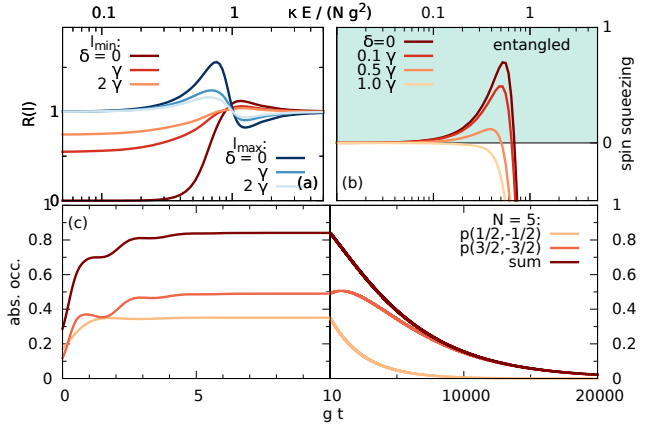


Figure 5. (a) The ratio $R(l)$ for $N = 5$ for $l = l_{min}, l_{max}$ and varying δ : The clear switching at the phase transition survives for $\delta \sim \gamma$. (b) Entanglement via spin squeezing inequalities: entanglement below the transition for $\delta < \gamma$. (c) Driving the system to the maximum subradiance point with subsequent relaxation to the ground state $N = 5, \delta = 0$: A cascade of dark states is generated. Total dark state occupation close to unity.

However the spin preserving case cannot model the effects of pure dephasing and the spin preserving and nonpreserving scenarios are two limits of the same physical system [42, 43]. Thus an investigation of entanglement in our setup and its preservation under dephasing is desirable: We find that the spin squeezing inequalities (SSI) by Tóth *et al.* detect entanglement below the phase transition for $\delta < \gamma$, see Fig. 5 (b) (see supplementary information for the SSI and a definition of the quantity in Fig. 5 (b)). Hence the entanglement detected in the spin preserving setup is still present for spin nonpreserving setups.

Super- and subradiance are concepts related to time evolution and so far we have only presented steady state values: Now, we drive the system to the steady state of maximum $R(l_{min})$ and then we switch off the driving field. The system relaxes into the ground state and we observe that a cascade of dark states is generated, Fig. 5 (c): $p(1/2, -1/2)$ and $p(3/2, -3/2)$ are the populations in the lowest states of the smallest $l = l_{min}$ and intermediate $l_{max} > l > l_{min}$ subspace, c.f. Fig. 1 (b). Both states are dark. They are populated on time scales g^{-1} , because the higher energy, bright states of the associated l subspaces decay via the emission of cavity photons, which subsequently leave the cavity through the cavity decay. After the initial fast population of these states due to the TLS cavity interaction the dynamics are governed by spontaneous emission. The overall dark state population subsequently decays on the slower time scale $\gamma^{-1} = 5000g^{-1}$ towards the ground state of the TLS ($|5/2, -5/2\rangle$). The decay follows the cascade $p(1/2, -1/2) \rightarrow p(3/2, -3/2) \rightarrow p(5/2, -5/2)$.

In general for different N : All $m > -l$ states relax to the $m = -l$ states on time scales of g^{-1} which is orders of magnitude faster than γ^{-1} . Subsequently the dark states $|l, -l\rangle$ relax in a cascade to the lower energy, dark states $|l+1, -l-1\rangle$ on time scales of γ^{-1} towards the ground state $|l_{max}, -l_{max}\rangle$, Fig. 1 (b). Please note that the overall occupation in subradiant dark states reaches values close to one. Subradiant correlations are clearly dominant here, since without these correlations the excitation in the TLS would still decay via the TLS cavity interaction Hamiltonian. This could be exploited for a controlled generation of subradiant states.

Experimental systems for observing these effects have to meet certain requirements: the pure dephasing of the TLS coherences should be small compared to the decay rate, i.e. $\delta \sim \gamma$. This can be realized at low temperatures with e.g. NV centers [44] or quantum dots [45]. Also a small inhomogeneous broadening is required, since it would likely blur the presented effect. For quantum dots this is more challenging than for NV centers. Generally, the decay rate γ is not a crucial parameter but the ratio between decay and pure dephasing. If pure dephasing is too large the steady state effects are blurred, in the ground state relaxation subradiant state occupation is decreased and coherence times are shorter.

The parameters used in this study are realistic for both NV centers and quantum dots and the behavior is stable over a wide parameter range.

In summary we have shown that the nonequilibrium phase transition of cooperative resonance fluorescence changes drastically when leaving the bad cavity limit: Subradiant Dicke states are amplified and clear experimental signatures of this effect emerge. Letting the system relax into the ground state generates a dark state cascade that can be utilized to store quantum information.

We thank N. Naumann for useful discussions, and gratefully acknowledge support from the Deutsche Forschungsgemeinschaft (DFG) through SFB 951 (M.G., M.R., A.K.) and through the School of Nanophotonics of the SFB 787 (M.G.) and BR 1528/8-2 (A.C., A.K.).

* michael.gegg@tu-berlin.de

- [1] R. H. Dicke, Phys. Rev. **93**, 99 (1954).
- [2] B. M. Garraway, Philos Trans A Math Phys Eng Sci **369**, 1137 (2011).
- [3] Y. K. Wang and F. T. Hioe, Phys. Rev. A **7**, 831 (1973).
- [4] D. F. Walls, P. D. Drummond, S. S. Hassan, and H. J. Carmichael, Suppl. Prog. Theor. Phys. **64**, 307 (1978).
- [5] H. J. Carmichael, J. Phys. B: At. Mol. Phys. **13**, 3551 (1980).
- [6] P. D. Drummond and D. F. Walls, Phys. Rev. A **23**, 2563 (1981).
- [7] S. Hassan, R. Bullough, R. Puri, and S. Lawande, Phys. A **103**, 213 (1980).
- [8] S. V. Lawande, R. R. Puri, and S. S. Hassan, J. Phys. B **14**, 4171 (1981).
- [9] C. Emary and T. Brandes, Phys. Rev. Lett. **90**, 044101 (2003).
- [10] S. Schneider and G. J. Milburn, Phys. Rev. A **65**, 042107 (2002).
- [11] L. Schneebeli, M. Kira, and S. W. Koch, Phys. Rev. Lett. **101**, 097401 (2008).
- [12] T. E. Lee, H. Häffner, and M. C. Cross, Phys. Rev. Lett. **108**, 023602 (2012).
- [13] A. González-Tudela and D. Porras, Phys. Rev. Lett. **110**, 080502 (2013).
- [14] Y. Su, D. Bimberg, A. Knorr, and A. Carmele, Phys. Rev. Lett. **110**, 113604 (2013).
- [15] C. Carr, R. Ritter, C. G. Wade, C. S. Adams, and K. J. Weatherill, Phys. Rev. Lett. **111**, 113901 (2013).
- [16] S. Genway, W. Li, C. Ates, B. P. Lanyon, and I. Lesanovsky, Phys. Rev. Lett. **112**, 023603 (2014).
- [17] L. J. Zou, D. Marcos, S. Diehl, S. Putz, J. Schmiedmayer, J. Majer, and P. Rabl, Phys. Rev. Lett. **113**, 023603 (2014).
- [18] M. Richter, M. Gegg, T. S. Theuerholz, and A. Knorr, Phys. Rev. B **91**, 035306 (2015).
- [19] E. Wolfe and S. F. Yelin, Phys. Rev. Lett. **112**, 140402 (2014).
- [20] M. O. Scully, Phys. Rev. Lett. **115**, 243602 (2015).
- [21] K. Cong, Q. Zhang, Y. Wang, G. T. Noe, A. Belyanin, and J. Kono, JOSA B **33**, C80 (2016).
- [22] P. Kirton and J. Keeling, Phys. Rev. Lett. **118**, 123602 (2017).
- [23] W. Guerin, M. O. Araújo, and R. Kaiser, Phys. Rev. Lett. **116**, 083601 (2016).
- [24] M. Gegg and M. Richter, New J. Phys. **18**, 043037 (2016).
- [25] S. Hartmann, Quantum Inf. Comput. **16**, 1333 (2016).
- [26] M. Xu, D. A. Tieri, and M. J. Holland, Phys. Rev. A **87**, 062101 (2013).
- [27] H.-P. Breuer and F. Petruccione, *The theory of open quantum systems* (Oxford, 2002).
- [28] L. Mandel and E. Wolf, *Optical coherence and quantum optics* (Cambridge, 1995).
- [29] H. M. Gibbs, *Optical Bistability: Controlling light with light* (Academic Press, 1985).
- [30] S. Rodriguez, W. Casteels, F. Storme, I. Sagnes, L. L. Gratiet, E. Galopin, A. Lemaitre, A. Amo, C. Ciuti, and J. Bloch, arXiv preprint arXiv:1608.00260 (2016).
- [31] S. Sarkar and J. S. Satchell, Europhys. Lett. **3**, 797 (1987).
- [32] A. Schenzle and H. Brand, Optics Communications **31**, 401 (1979).
- [33] E. M. Kessler, G. Giedke, A. Imamoglu, S. F. Yelin, M. D. Lukin, and J. I. Cirac, Phys. Rev. A **86**, 012116 (2012).
- [34] M. Gegg and M. Richter, “Psiquasp,” release under preparation (2017).
- [35] S. Balay, S. Abhyankar, M. F. Adams, J. Brown, P. Brune, K. Buschelman, L. Dalcin, V. Eijkhout, W. D. Gropp, D. Kaushik, M. G. Knepley, L. C. McInnes, K. Rupp, B. F. Smith, S. Zampini, H. Zhang, and H. Zhang, “PETSc Web page,” <http://www.mcs.anl.gov/petsc> (2017).
- [36] S. Balay, S. Abhyankar, M. F. Adams, J. Brown, P. Brune, K. Buschelman, L. Dalcin, V. Eijkhout, W. D. Gropp, D. Kaushik, M. G. Knepley, L. C. McInnes, K. Rupp, B. F. Smith, S. Zampini, H. Zhang, and H. Zhang, *PETSc Users Manual*, Tech. Rep. ANL-95/11

- Revision 3.7 (Argonne National Laboratory, 2016).
- [37] S. Balay, W. D. Gropp, L. C. McInnes, and B. F. Smith, in *Modern Software Tools in Scientific Computing*, edited by E. Arge, A. M. Bruaset, and H. P. Langtangen (Birkhäuser Press, 1997) pp. 163–202.
- [38] V. Hernandez, J. E. Roman, and V. Vidal, ACM Trans. Math. Software **31**, 351 (2005).
- [39] M. Richter, T. Renger, G. Renger, and A. Knorr, J. Chem. Phys. **127**, 075105 (2007).
- [40] P. R. Rice and H. J. Carmichael, Phys. Rev. A **50**, 4318 (1994).
- [41] D. H. E. Gross, *Microcanonical Thermodynamics: Phase Transitions in "Small" Systems* (World Scientific, 2001).
- [42] G. S. Agarwal, Springer Tr. Mod. Phys. **74**, 25 (1974).
- [43] H. J. Carmichael, *Statistical Methods in Quantum Optics I: Master Equations and Fokker-Planck Equations* (Springer, 2002).
- [44] P. Tamarat, T. Gaebel, J. R. Rabeau, M. Khan, A. D. Greentree, H. Wilson, L. C. L. Hollenberg, S. Prawer, P. Hemmer, F. Jelezko, and J. Wrachtrup, Phys. Rev. Lett. **97**, 083002 (2006).
- [45] P. Borri, W. Langbein, S. Schneider, U. Woggon, R. L. Sellin, D. Ouyang, and D. Bimberg, Phys. Rev. Lett. **87**, 157401 (2001).